 CMC, vol.60, no.1, pp.335-349, 2019

A Novel Broadband Microstrip Antenna Based on Operation of Multi-Resonant Modes

Taohua Chen[1], Yueyun Chen[1,*], Rongling Jian[1], Zushen Liu[2] and Alan Yang[3]

Abstract: A novel broadband microstrip antenna under operation of $TM_{1/2,0}$, TM_{10} and TM_{12} modes through a shorting wall and slots is proposed in this paper. Initially, an inverted U-shaped slot is adopted around the feeding point, which achieves a good impedance matching on TM_{10} mode and separates the patch into two parts. Additionally, a shorting wall is added underneath the edge of smaller patch to excite another one-quarter resonant mode, i.e., $TM_{1/2,0}$ mode of smaller patch close to TM_{10} mode to expand the impedance bandwidth. Further, the antenna width is enlarged and two symmetrical vertical rectangular slots are cut on the patch to reduce the frequency of TM_{12} mode to form a broadband. Based on the arrangements above, a wide impedance bandwidth with three minima can finally be achieved. The results show that the impedance bandwidth of proposed antenna for $|S_{11}|$<-10 dB is extended to 26.5% (23.5-30.67 GHz), which is three times of the conventional antenna at same profile. Moreover, a stable radiation pattern at broadside direction is realized over the operating band.

Keywords: Broadband, microstrip antenna, shorting wall, slots, three resonant modes.

1 Introduction

With the development of modern communication systems, microstrip antenna (MSA) has attracted much attention in wireless communication because of their low profile, small cost, and ease of manufacture [Chen, Jian, Ma et al. (2017)]. However, conventional MSA always suffers from a narrow impedance bandwidth, usually less than 3% [Sun, Li, Zhang et al. (2017)]. Thus, how to extend the bandwidth of MSA effectively becomes a hot research topic in recent years.

Several methods have been proposed to improve the impedance bandwidth of MSA. The simplest method to expand bandwidth is enhancing the antenna thickness and decreasing the substrate permittivity [Constantine (2005)]. However, using thick substrates will enlarge the surface wave leakage leading to a decrease in radiation efficiency and the lowest substrate dielectric constant is 1, i.e., air.

Additionally, in Liao et al. [Liao, Xue and Xu (2012)], the feeding scheme was reconfigured to extend the impedance bandwidth to 115% by introducing another non

[1] University of Science & Technology Beijing, Beijing, 100083, China.

[2] The 41st Institute of China Electronics Technology Group Corporation, Bengbu, 233006, China.

[3] Amphenol AssembleTech, Houston, 77070, United States.

[*] Corresponding Author: Yueyun Chen. Email: chenyy@ustb.edu.cn.

resonant mode around the fundamental mode. In addition, the L-shaped and F-shaped probe feeds in Mak et al. [Mak, Lai and Luk (2018); Jin and Du (2015)] was adopted to enhance the bandwidth to 54% and 45%, respectively. The reason for bandwidth enhancement of these antennas is that the changed probes can eliminate the impedance inductance to make a great impedance matching. Nevertheless, it is difficult to implement the feeding scheme in a thin substrate.

Moreover, slotting on the patch is another effective method, which was widely used in the past decades to expand the impedance bandwidth because of the simple implementation. The authors in Huynh et al. [Huynh and Lee (1995)] proposed a U-shaped slot on the radiating patch to extend the impedance bandwidth to 47%. When a U-shaped slot was adopted, the frequencies of higher-order modes were reduced to around that of fundamental mode to achieve a broadband [Deshmukh and Ray (2015)]. Besides, in Yang et al. [Yang, Zhang, Ye et al. (2001)], a simple E-shaped microstrip patch was proposed. The antenna in Yang et al. [Yang, Zhang, Ye et al. (2001)] could exist two different current paths by two symmetrical vertical rectangular slots cut on the patch, which realized the combination of two resonant modes and enhanced the bandwidth to 30.3%. And in Deshmukh et al. [Deshmukh and Ray (2009)], the antenna bandwidth was extended to 24.6% by adopting a half U-shaped slot on the semi E-shaped antenna. Also, wang-shaped patch in Chung et al. [Chung and Wong (2010)], modified E-shaped patch in Koutinos et al. [Koutinos, Anagnostou, Joshi et al. (2018)] and modified U-slotted antenna in Costanzo et al. [Costanzo and Costanzo (2013)] were proposed for bandwidth enhancement. However, the all antennas with slots loaded on the patch mentioned above are high-profile antennas, which destroys the low-profile property of microstrip antenna.

Furthermore, in recent years, coupling two odd modes of MSA together becomes a new attractive method. The TM_{10} and TM_{30} modes could be combined together to achieve bandwidth enhancement by shorting pins and slots, and the bandwidth was increased to 13%, 18% and 11.8% in Liu et al. [Liu, Zhu and Choi (2017)], Wang et al. [Wang, Ng, Chan et al. (2015)] and Liu et al. [Liu, Zhu, Choi et al. (2017)], respectively. In Liu et al. [Liu, Zhu, Choi et al. (2018); Liu, Zhu and Choi (2017)], through same method to combine TM_{10} and TM_{12} modes, the impedance bandwidth was increased to 10% and 15.3%, respectively. However, since only two odd modes are combined, the impedance bandwidth of these antennas are only twice as wide as that of traditional microstrip antennas, which may hinder the application of these MSAs in broadband communication systems.

In this paper, a novel patch antenna under operation of $TM_{1/2,0}$, TM_{10} and TM_{12} modes through a shorting wall and slots is proposed to achieve bandwidth expansion. Firstly, an inverted U-shaped slot is loaded around the feeding point on the patch to achieve a good impedance matching and separates the patch into two parts. Secondly, a shorting wall is added underneath the smaller patch produced by the inverted U-shaped slot, which will excite another resonant mode, i.e., $TM_{1/2,0}$ of smaller patch antenna close to TM_{10} mode to expand the impedance bandwidth. Thirdly, to further extend the bandwidth, the antenna width is enlarged and two symmetrical vertical rectangular slots is cut on the patch to reduce the frequency of TM_{12} mode to form a broadband. Finally, a broadband of 26.5% (23.5-30.67 GHz) for $|S_{11}| < -10$ dB is achieved and the impedance bandwidth is three times that of conventional antenna at same profile. Moreover, a stable radiation

pattern at the broadside direction is realized over the operating band. In this paper, full-wave simulation software HFSS 13.0 is used for simulation calculation.

2 Antenna configuration and design process

2.1 Antenna configuration

The configuration of the proposed broadband microstrip antenna is shown in Fig. 1. It consists of a rectangular radiating patch with the size of $L\times W$, a ground plane with the size of $L_s\times W_s$, an inverted U-shape slot with the width of W_2, two symmetrical vertical rectangular slots with the size of $L\times W_1$ and a shorting wall with the dimensions of $W_3\times H$ which is L_3 distance from the lower edge of patch. Between the patch and the ground, a dielectric substrate RO5880 with a permittivity of ε_r=2.2 and a thickness of H=0.787 mm is selected in this paper for antenna design. And all parameters for the proposed broadband antenna in Fig. 1 are tabulated in Tab. 1.

Firstly, the inverted U-shaped slot is adopted to achieve impedance matching of the traditional antenna and separates the patch into two parts. Secondly, a shorting wall is added to connect the smaller patch and ground to excite a one-quarter wavelength resonant mode, i.e., $TM_{1/2,0}$ of the smaller patch to expand the impedance bandwidth. To further extend the bandwidth, the antenna width is enlarged and two symmetrical vertical rectangular slots are cut on the patch to reduce the frequency of TM_{12} mode. Finally, a wideband antenna can be realized with three minima in operating band.

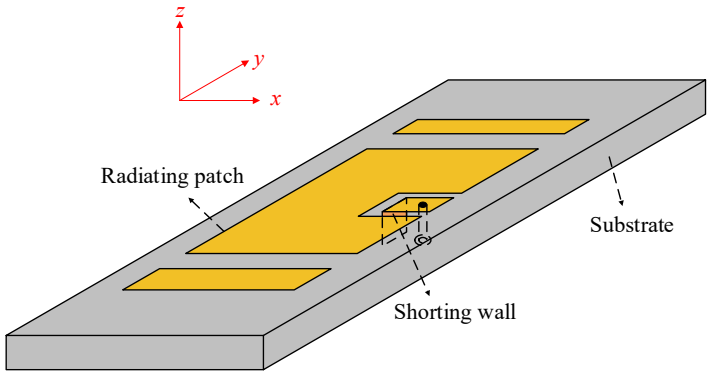

(a)

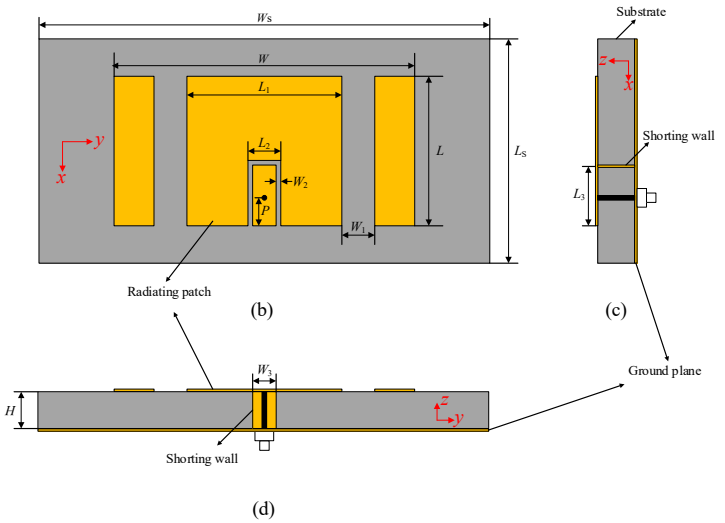

Figure 1: Configuration of the proposed broadband antenna loaded with a shorting wall and slots (a) 3D view. (b) Top view. (c) Right view. (d) Front view

Table 1: Dimensions of the proposed broadband antenna in Fig. 1 (mm)

L_S	L	L_1	L_2	L_3	W_s	W	W_1	W_2	P	H
4.8	3.2	3.3	0.54	1.3	9.6	6.4	1	0.04	0.92	0.787

2.2 Design process

In order to expand the impedance bandwidth of microstrip antenna, the structure of traditional microstrip antenna is modified. The design process of proposed broadband antenna is shown in Fig. 2.

Initially, the ANT 1 is an inverted U-shaped slot cut around the feeding point on the radiating patch of the conventional antenna to achieve impedance matching. Then, for the ANT 2, another resonant mode near TM_{10} mode is excited through a shorting wall added underneath the edge of smaller patch produced by the inverted U-shaped slot. To further expand the impedance bandwidth, for the ANT 3, i.e., proposed antenna, the antenna width is enlarged and two symmetrical vertical rectangular slots are cut on the patch to reduce the frequency of TM_{12} mode close to that of TM_{10} mode. The radiating patches of ANT 1 and ANT 2 are with the same size (W=1.5 L), and the patch width of ANT 3 is enlarged to twice of the length. The simulated reflection coefficients are shown in Fig. 3. The antennas dimensions are optimized to good impedance matching. It can be observed from the Fig. 3 that the impedance bandwidth for $|S_{11}|$<-10 dB of ANT 1 is 9.4% (24.17-26.55 GHz), and is 18.4% (23.45-28.2 GHz) for ANT 2. The reason of enhancement of the impedance bandwidth is that another resonant mode, i.e., $TM_{1/2,0}$ mode which is excited through a shorting wall underneath the smaller patch produced by the inverted U-shaped slot is coupled to the fundamental TM_{10} mode. As for the proposed antenna ANT 3, the impedance bandwidth is further extended to 26.5% (23.5-30.67 GHz). Through two

symmetrical vertical rectangular slots and increasing the patch width to twice of the length, for ANT 3, another resonant mode, i.e., TM_{12} mode is added to form a wider bandwidth, which can be easily observed from Fig. 3.

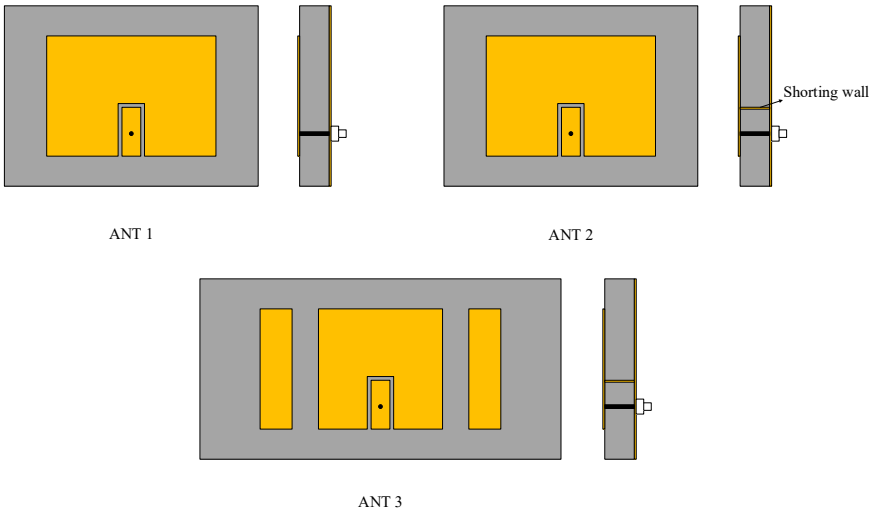

Figure 2: Design process of proposed antenna

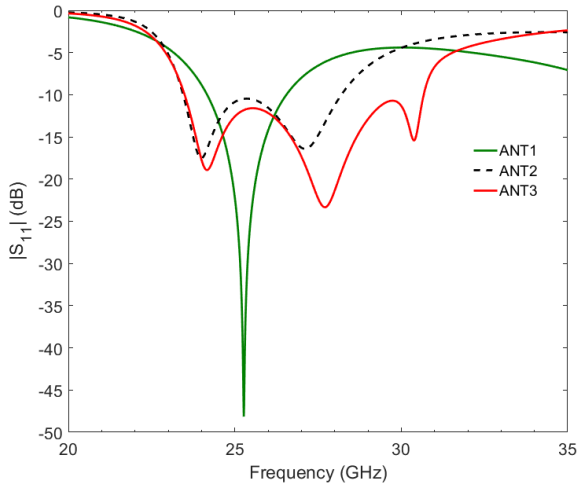

Figure 3: Simulated reflection coefficients of three antennas

2.3 Operating mechanism

To understand the operating mechanism of the proposed antenna, Fig. 4 plots the electric field distributions of the radiating patch. For the electric field distributions at 24.18 GHz, the electric field is mainly distributed at lower edge of the smaller patch around the feeding point, which is similar to the one-quarter wavelength resonant mode, i.e., $TM_{1/2,0}$ mode of smaller patch. While at the 27.74 GHz, the electric field distributions are similar

to the fundamental TM_{10} mode which is mainly distributed at the edge of conventional patch. In addition, for the 30.39 GHz, the electric field is mainly distributed at the patches on left and right sides produced by two symmetrical vertical rectangular slots. Compared with the electric field distributions of TM_{12} mode in the patch without rectangular slots, the rectangular slots destroy the electric field distributions, which will reduce the frequency of TM_{12} mode. Though coupling the three resonant modes together, a broadband microstrip antenna can be realized.

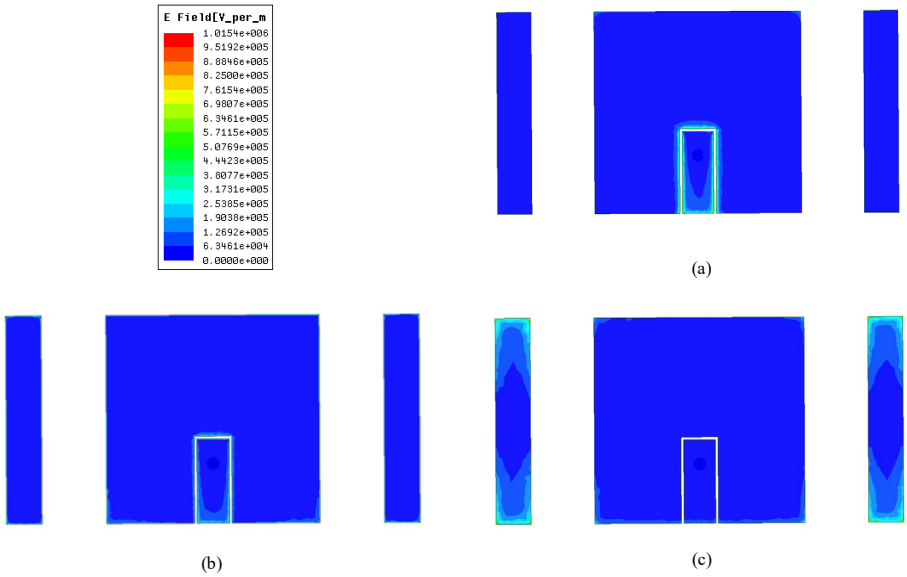

Figure 4: Simulated electric field distributions of proposed antenna. (a) 24.18 GHz. (b) 27.74 GHz. (c) 30.39 GHz

2.4 Reducing the resonant frequency of TM_{12} mode

In order to better illustrate how to reduce the frequency of TM_{12} mode, the specific analysis is made in this subsection. According to the cavity model [Garg, Bhartia, Bahl et al. (2001)], the resonant frequencies (f_{mn}) of TM_{mn} modes in microstrip antenna can be expressed as follows:

$$f_{mn} = \frac{c}{2\sqrt{\varepsilon_r}} \times \sqrt{\left(\frac{m}{L}\right)^2 + \left(\frac{n}{W}\right)^2} \tag{1}$$

where c is the light speed in the free space, ε_r is the dielectric constant of substrate, and m=1, 2, 3 … and n=1, 2, 3 …

Based on formula (1), the patch width (W) plays an important role in the frequency of TM_{12} mode (f_{12}), yet has no effect on that of TM_{10} mode (f_{10}). Therefore, when W is increased, f_{12} will be reduced while f_{10} keeps constant. In this paper, considering the antenna size, the patch width is enlarged to twice of the length. However, when patch

width is twice of length, the distance of f_{10} and f_{12} is still large, which cannot to form a wide bandwidth. Thus, two symmetrical vertical rectangular slots are cut on the patch to further reduce f_{12}.

Initially, four symmetrical vertical rectangular slots are loaded on the patch, which can be observed at Fig. 5.

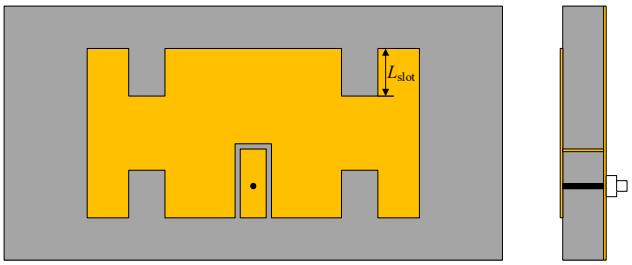

Figure 5: Antenna with four symmetrical vertical rectangular slots

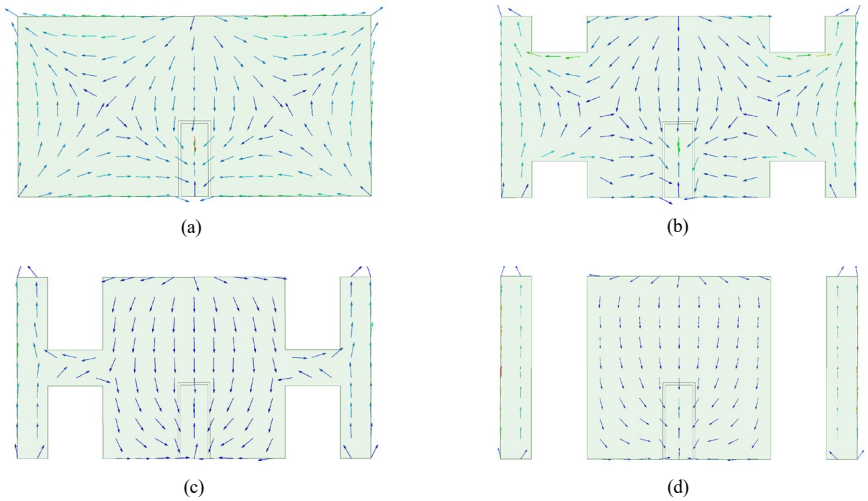

Figure 6: Current distribution of TM_{12} mode at different slots length. (a) Without slots, 39.57 GHz. (b) L_{slot}=0.2L, 36.17 GHz. (c) L_{slot}=0.4L, 31.27 GHz. (d) L_{slot}=0.5L, 30.26 GHz

Because the four vertical rectangular slots are parallel to current flow direction of TM_{10} mode, they have little effect on f_{10}. However, for the TM_{12} mode, the slots enlarge the horizontal current path, which will reduce the f_{12}. To better understand the effects of four symmetrical vertical rectangular slots on TM_{12} mode, the current distribution of TM_{12} mode at different slots length is plotted on Fig. 6, and the other antenna parameters are fixed as shown in Tab. 1.

It can be clearly seen from Fig. 6 that the slots length has great effect on the TM_{12} current path corresponding to f_{12}. Moreover, Fig. 6 also gives the f_{12} at different slots length, we can find that the f_{12} decreases from 39.57 GHz to 30.26 GHz as the slots length increases from 0 to 0.5L. Moreover, to better show the effect of slots length on f_{10}

and f_{12}, Fig. 7 plots the f_{10} and f_{12} varying with the slots length when other parameters are fixed. As can be observed from Fig. 7, the f_{10} keeps stable while f_{12} decreases as the slots length increases, as predicted above.

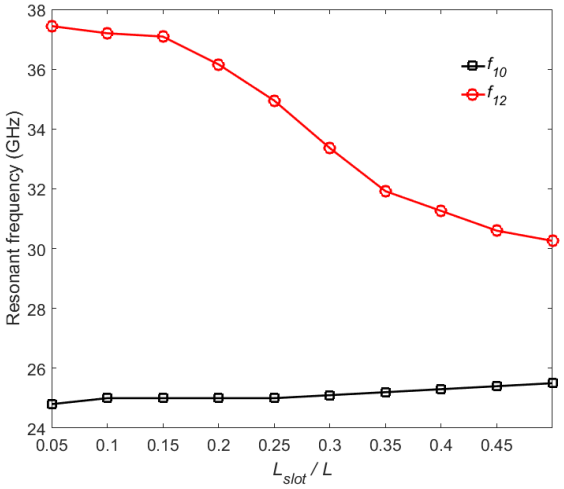

Figure 7: f_{10} and f_{12} varying with the slots length L_{slot}

Finally, considering the all antenna performances, we select $L_{\text{slot}} = 0.5L$ in this paper and for this reason there are only two large symmetrical vertical rectangular slots at last. Note that the TM_{02} mode between TM_{10} and TM_{12} modes is removed when $L_{\text{slot}} = 0.5L$ is adopted, and the radiation peak of TM_{12} mode is changed to boresight because of the slots [Xiao, Wang, Shao et al. (2005)].

3 Parametric studies

To deeply understand how the influence of dimensional parameters on the proposed antenna performances and design flow, parametric studies for the proposed wideband antenna is carried out by using HFSS 13.0. In this paper, several key parameters listed in Tab. 1 are extensively studied under other parameters to be fixed.

3.1 Effects of two symmetrical vertical rectangular slots position L_1 and width W_1

Fig. 8 plots the simulated results of the $|S_{11}|$ as a function of frequency at different symmetrical vertical rectangular slots position L_1. As can be observed from the Fig. 8, compared with the third resonant mode, i.e., TM_{12} mode, the first resonant mode ($TM_{1/2,0}$ mode) and second resonant mode (TM_{10} mode) are less influenced by the vertical rectangular slots position L_1. The reason is that two symmetrical vertical rectangular slots cut off the horizontal current of TM_{12} mode, while have little effect on the vertical current of $TM_{1/2,0}$ and TM_{10} modes. When L_1 is from 3.1 mm to 3.5 mm, the impedance matching of TM_{12} mode becomes better gradually and the frequency of TM_{12} mode increases. Yet, when L_1=3.5 mm, the band between TM_{10} and TM_{12} mode becomes mismatched, and the best bandwidth can be obtained at L_1=3.3 mm from Fig. 8.

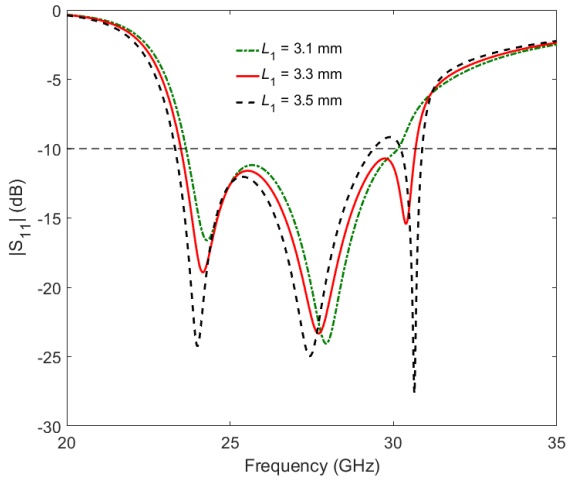

Figure 8: $|S_{11}|$ as a function of frequency at different L_1

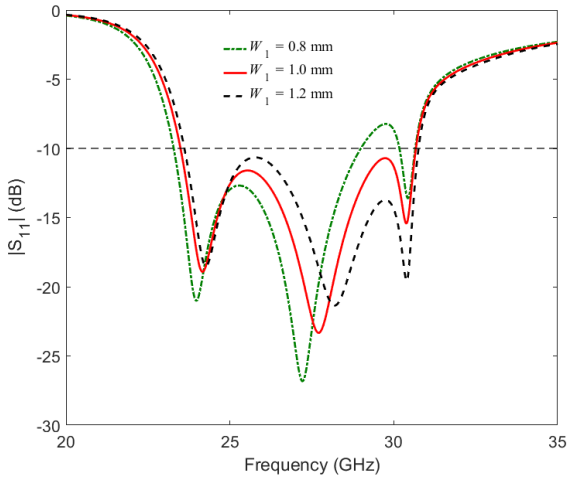

Figure 9: $|S_{11}|$ as a function of frequency at different W_1

In Fig. 9, the $|S_{11}|$ as a function of frequency at different vertical rectangular slots width W_1 is illustrated. Like L_1, the W_1 has little effect on the $TM_{1/2,0}$ mode. However, the W_1 begins to affect TM_{10} and TM_{12} modes concurrently. The wider the W_1, the closer the distance between TM_{10} and TM_{12} modes. And the widest bandwidth can be seen at W_1=1.0 mm from Fig. 9.

3.2 Effects of smaller patch length L_3 and width W_3

Fig. 10 gives the $|S_{11}|$ as a function of frequency at different smaller patch length L_3. As expected, the L_3 has a great impact on the $TM_{1/2,0}$ mode. When L_3 increases from 1.2 mm to 1.4 mm, the frequency of $TM_{1/2,0}$ corresponding to the L_3 decreases. Meanwhile, the L_3

affects the impedance matching of all three modes. And the best value of L_3 can be found from Fig. 10 is L_3 =1.3 mm.

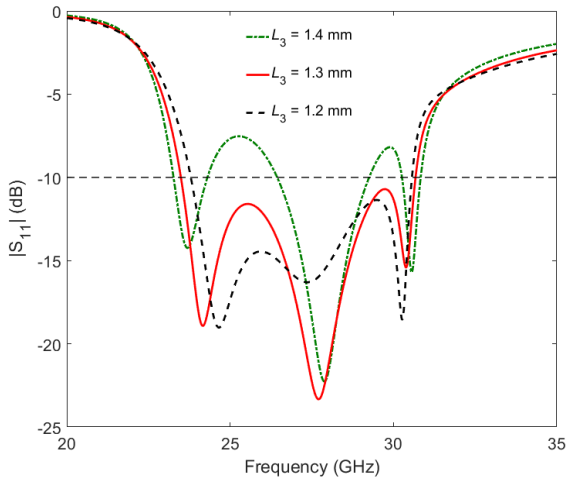

Figure 10: $|S_{11}|$ as a function of frequency at different L_3

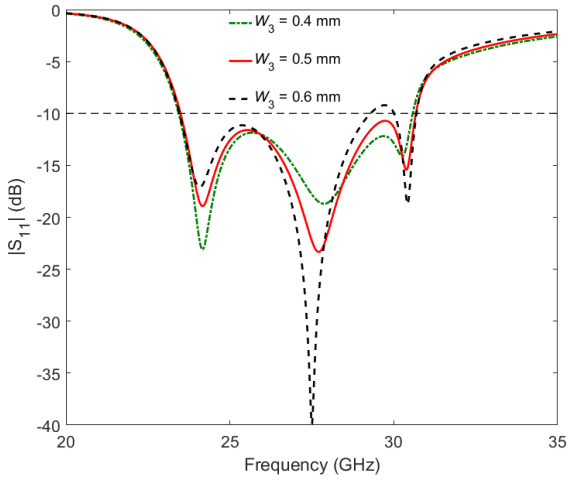

Figure 11: $|S_{11}|$ as a function of frequency at different W_3

Fig. 11 shows the $|S_{11}|$ as a function of frequency at different smaller patch width W_3. The W_3 mainly affects the impedance matching of three resonant modes and has little influence on the resonant frequencies of three modes. Considering the whole $|S_{11}|$ performance in Fig. 11, the W_3=0.5 mm is selected in this paper.

3.3 Effects of inverted U-shaped slot width W_2 and feeding position P

Fig. 12 and Fig. 13 plot the $|S_{11}|$ as a function of frequency at different inverted U-shaped slot width W_2 and feeding position P, respectively.

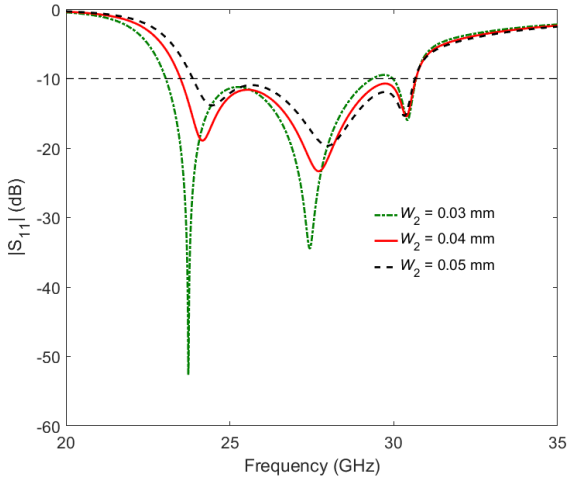

Figure 12: $|S_{11}|$ as a function of frequency at different W_2

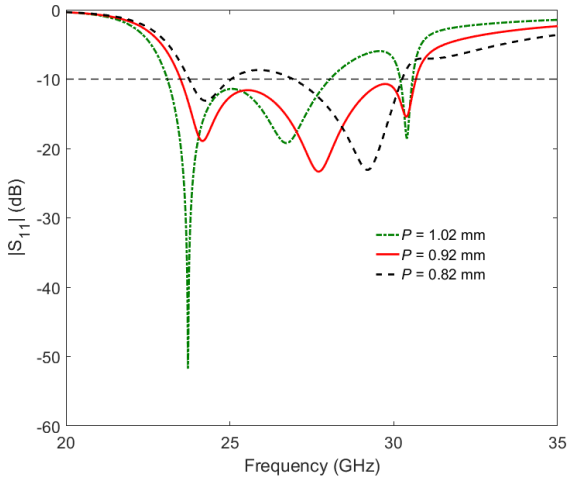

Figure 13: $|S_{11}|$ as a function of frequency at different P

As can be observed from Fig. 12, the W_2 mainly influences the impedance matching of $TM_{1/2,0}$ and TM_{10} modes. And best $|S_{11}|$ performance of $TM_{1/2,0}$ and TM_{10} modes is achieved at W_2=0.03 mm. However, the band between TM_{10} and TM_{12} mode is mismatched at W_2=0.03 mm. Thus, considering the whole $|S_{11}|$ performance, in this paper, W_2=0.04 mm is selected. For the feeding position P, as can be seen from Fig. 13, it has great effects on the matching condition. Moreover, the best value of P is realized at P=0.92 mm.

4 Results and discussion

The reflection coefficient of proposed broadband microstrip antenna is plotted in Fig. 14.

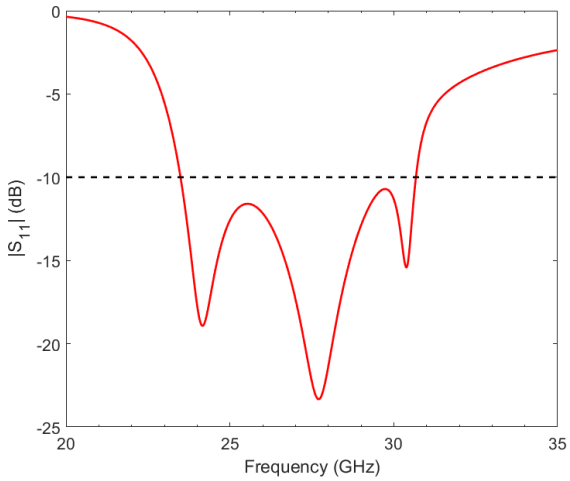

Figure 14: $|S_{11}|$ of proposed broadband antenna

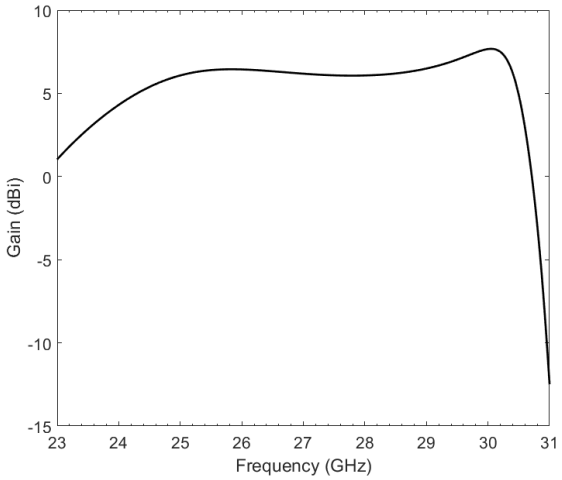

Figure 15: Gain at broadside direction of proposed antenna

It can be observed from Fig. 14 that the impedance bandwidth for $|S_{11}|$<-10 dB is extended to 26.5%, ranging from 23.5 to 30.67 GHz. Meanwhile, there are three minima in the operating band, which is consistent with the three resonant modes mentioned above. Compared with the conventional antenna bandwidth of 9.4% at the same profile, the impedance bandwidth of proposed antenna is about three times that of the conventional antenna through coupling three resonant modes together.

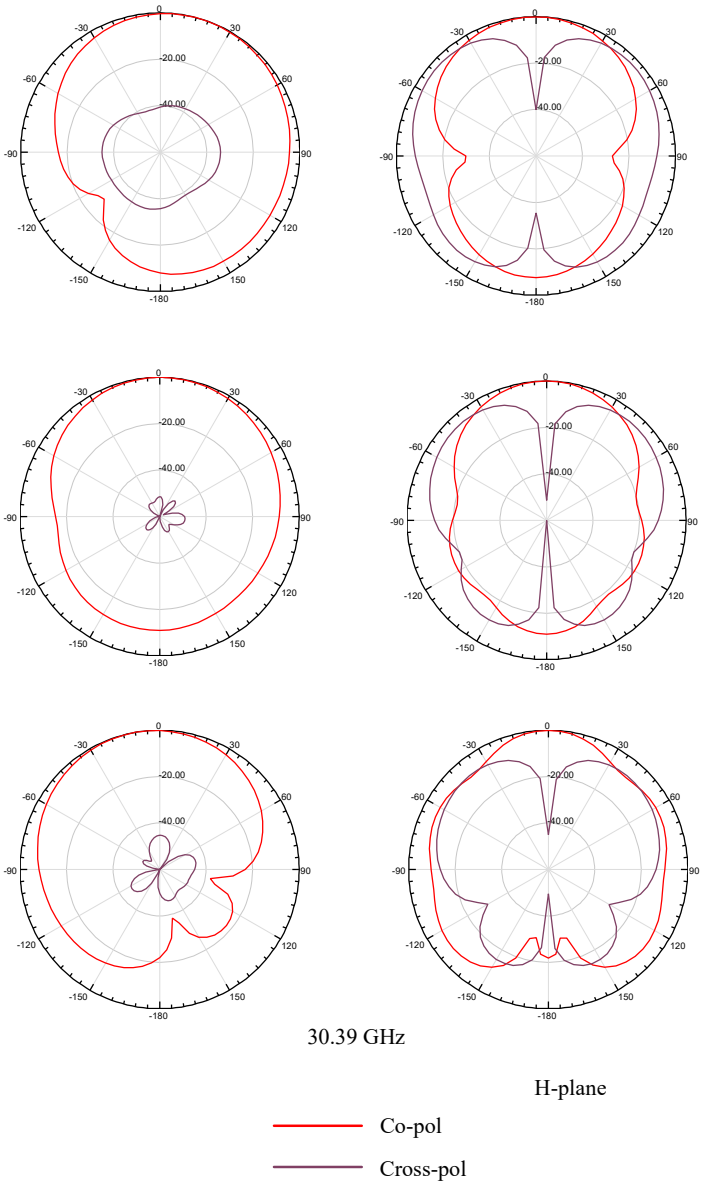

Figure 16: Normalized radiation patterns of proposed antenna at 24.18, 27.74 and 30.39 GHz

Moreover, the gain as a function of frequency at broadside direction of proposed antenna is illustrated in Fig. 15. It can be seen from Fig. 15 that the proposed antenna has obtained a stable gain of around 6 dBi at the broadside direction in the operating band, which shows that the proposed wideband antenna has a good gain performance in the operating band.

Fig. 16 gives the normalized radiation patterns of proposed antenna at three minima of 24.18, 27.74 and 30.39 GHz. As for the E-plane, the co-polarization radiation patterns are a little asymmetric because of the asymmetric antenna structure. Yet, it is still stable at

the operating band. Meanwhile, the cross-polarization level in E-plane is lower than -30 dB over the operating band, which indicates that the proposed broadband antenna has a good radiation performance in E-plane. While for the H-plane, the co-polarization radiation patterns are symmetric, and the cross-polarization level in the broadside direction is lower than -40 dB over the operating band.

5 Conclusion

In this paper, a novel broadband microstrip antenna is proposed and analyzed. A shorting wall is adopted to excite a one-quarter resonant mode ($TM_{1/2,0}$ mode) close to the fundamental mode (TM_{10} mode) to expand the impedance bandwidth. Further, through two symmetrical vertical rectangular slots and enlarging the antenna width to twice of the length, the TM_{12} mode is also adjusted in proximity to the TM_{10} mode. Finally, a broadband microstrip antenna with impedance bandwidth of 26.5% for $|S_{11}|$<-10 dB is achieved, and its bandwidth is about three times of the conventional antenna at same profile. In addition, a stable radiation pattern at the broadside direction is realized over the operating band. The proposed antenna is compact and wideband, it can be used for 5G wireless communication in the future.

Acknowledgement: This work was supported by National Science and Technology Major Project No. 2017ZX03001021-005.

References

Chen, Y. Y.; Jian, R. L.; Ma, S. S.; Mohadeskasaei, S. A. (2017): A research for millimeter wave patch antenna and array synthesis. *IEEE Wireless and Optical Communication Conference*, pp. 1-5.

Chung, K. L.; Wong, C. H. (2010): Wang-shaped patch antenna for wireless communications. *IEEE Antennas & Wireless Propagation Letters*, vol. 9, no. 1, pp. 638-640.

Constantine, A. B. (2005): *Antenna Theory: Analysis and Design.* John Wiley & Sons, USA.

Costanzo, S.; Costanzo, A. (2013): Compact U-slotted antenna for broadband radar applications. *Journal of Electrical and Computer Engineering*, vol. 2013, pp. 10.

Deshmukh, A. A.; Ray, K. P. (2009): Compact broadband slotted rectangular microstrip antenna. *IEEE Antennas & Wireless Propagation Letters*, vol. 8, no. 4, pp. 1410-1413.

Deshmukh, A.; Ray, K. P. (2015): Analysis of broadband variations of U-slot cut rectangular microstrip antennas. *IEEE Antennas and Propagation Magazine*, vol. 57, no. 2, pp. 181-193.

Garg, R.; Bhartia, P.; Bahl, I.; Ittipiboon, A. (2001): *Microstrip Antenna Design Handbook*. Artech House, UK.

Huynh, T.; Lee, K. F. (1995): Single-layer single-patch wideband microstrip antenna. *Electronics Letters*, vol. 31, no. 16, pp. 1310-1312.

Jin, Y.; Du, Z. (2015): Broadband dual-polarized F-probe fed stacked patch antenna for base stations. *IEEE Antennas & Wireless Propagation Letters*, vol. 14, pp. 1121-1124.

Koutinos, A. G.; Anagnostou, D. E.; Joshi, R.; Podilchak, S. K.; Kyriacou, G. A. et al.

(2018): Modified easy to fabricate E-shaped compact patch antenna with wideband and multiband functionality. *IET Microwaves, Antennas & Propagation*, vol. 12, no. 3, pp. 326-331.

Liao, S. W.; Xue, Q.; Xu, J. H. (2012): Parallel-plate transmission line and L-plate feeding differentially driven H-slot patch antenna. *IEEE Antennas & Wireless Propagation Letters*, vol. 11, no. 8, pp. 640-644.

Liu, N. W.; Zhu, L.; Choi, W. W. (2017): A differential-fed microstrip patch antenna with bandwidth enhancement under operation of TM_{10} and TM_{30} modes. *IEEE Transactions on Antennas and Propagation*, vol. 65, no. 4, pp. 1607-1614.

Liu, N. W.; Zhu, L.; Choi, W. W. (2017): A low-profile wide-bandwidth planar inverted-F antenna under dual resonances: principle and design approach. *IEEE Transactions on Antennas and Propagation*, vol. 65, no. 10, pp. 5019-5025.

Liu, N. W.; Zhu, L.; Choi, W. W.; Zhang, X. (2017): Wideband shorted patch antenna under radiation of dual resonant modes. *IEEE Transactions on Antennas and Propagation*, vol. 65, no. 6, pp. 2789-2796.

Liu, N. W.; Zhu, L.; Choi, W. W.; Zhang, X. (2018): A low-profile differential-fed patch antenna with bandwidth enhancement and sidelobe reduction under operation of TM_{10} and TM_{12} modes. *IEEE Transactions on Antennas and Propagation*, vol. 66, no. 9, pp. 4854-4859.

Mak, K. M.; Lai, H. W.; Luk, K. M. (2018): A 5G wideband patch antenna with antisymmetric L-shaped probe feeds. *IEEE Transactions on Antennas and Propagation*, vol. 66, no. 2, pp. 1-1.

Sun, W.; Li, Y.; Zhang, Z.; Feng, Z. (2017): Broadband and low-profile microstrip antenna using strip-slot hybrid structure. *IEEE Antennas and Wireless Propagation Letters*, vol. 16, no. 99, pp. 3118-3121.

Wang, D.; Ng, K. B.; Chan, C. H.; Wong, H. (2015): A novel wideband differentially-fed higher-order mode millimeter-wave patch antenna. *IEEE Transactions on Antennas and Propagation*, vol. 63, no. 2, pp. 466-473.

Xiao, S. Q.; Wang, B. Z.; Shao, W.; Zhang, Y. (2005): Bandwidth-enhancing ultralow-profile compact patch antenna. *IEEE Transactions on Antennas and Propagation*, vol. 53, no. 11, pp. 3443-3447.

Yang, F.; Zhang, X. X.; Ye, X.; Rahmat-Samii, Y. (2001): Wide-band E-shaped patch antennas for wireless communications. *IEEE Transactions on Antennas and Propagation*, vol. 49, no. 7, pp. 1094-1100.